Journal of the Korean Crystal Growth and Crystal Technology
Vol. 17, No. 6 (2007) 231-237

Essence of thermal convection for physical vapor transport of mercurous chloride in regions of high vapor pressures

Geug-Tae Kim†, Kyong-Hwan Lee* and Jeong-Gil Choi

Department of Nano-Bio Chemical Engineering, Hannam University, Daejeon 305-811, Korea
**Fossil Energy Environment Research Department, Korea Institute of Energy Research, Taejon 305-343, Korea*

(Received October 12, 2007)
(Accepted October 29, 2007)

Abstract For an aspect ratio (transport length-to-width) of 5, Pr = 3.34, Le = 0.078, Pe = 4.16, Cv = 1.01, P_B = 50 Torr, only thermally buoyancy-driven convection ($Gr = 4.83 \times 10^5$) is considered in this study in spite of the disparity in the molecular weights of the component A (Hg_2Cl_2) and B which would cause thermally and/or solutally buoyancy-driven convection. The crystal growth rate and the maximum velocity vector magnitude are decreased exponentially for $3 \le Ar \le 5$, for (1) adiabatic walls and (2) the linear temperature profile, with a fixed source temperature. This is related to the finding that the effects of side walls tend to stabilize convection in the growth reactor. The rate for the linear temperature profiles walls is slightly greater than for the adiabatic walls for varied temperature differences and aspect ratios. With the imposed thermal profile, a fixed source region, both the rate and the maximum velocity vector magnitude increase linearly with increasing the temperature difference for $10 \le \Delta T \le 50$ K.

Key words Mercurous chloride, Thermal convection, Aspect ratio, Physical vapor transport

1. Introduction

Interest in growing mercurous chloride (Hg_2Cl_2) single crystal stems from their exceptional optical broad transmission range from 0.36 to 20 μm for applications in acousto-optic and opto-electronic devices such as Bragg cells, X-ray detectors operating at ambient temperature [1]. The equimolar Hg_2Cl_2 compound decomposes to two liquids at a temperature near 525°C where the vapor pressure is well above 20 atm [2, 3]. Because of this decomposition and high vapor pressure, Hg_2Cl_2 cannot be solidified as a single crystal directly from the stoichiometric melt. However, very similar to the mercurous bromide, mercurous chloride exhibits sufficiently high vapor pressure at low temperatures so that these crystals are usually grown by the physical vapor transport (PVT) in closed silica glass ampoules. The PVT processing has many advantages over melt-growth methods since it can be conducted at low temperatures: (1) vapor-solid interfaces possess relatively high interfacial morphological stability against non-uniformities in heat and mass transfer; (2) high purity crystals are achieved; (3) materials decomposed before melting, such as Hg_2Cl_2 can be grown; (4) lower point defect and dislocation densities are achieved [4]. The mechanism of the PVT process is simple: sublimation-condensation in closed silica glass ampoules in temperature gradient imposed between the source material and the growing crystal. In the actual PVT system of Hg_2Cl_2, the molecular species Hg_2Cl_2 sublimes as the vapor phase from the crystalline source material (Hg_2Cl_2), and is subsequently transported and re-incorporated into the single crystalline phase (Hg_2Cl_2) [5]. Recently PVT has become an important crystal growth process for a variety of acousto-optic materials. However, the industrial applications of the PVT process remain limited. One of important main reasons is that transport phenomena occurring in the vapor are complex and coupled so that it is difficult to design or control the process accurately. Such complexity and coupling are associated with the inevitable occurrence of thermal and/or solutal convection generated by the interaction of gravity with density gradients arising from temperature and/or concentration gradients. In general, convection has been regarded as detrimental and, thus, to be avoided or minimized in PVT growth system. These thermal/and or soultal convection-induced complications result in problems ranging from crystal inhomogeneity to structural imperfection. Therefore, in order to analyze and control the PVT process accurately, and also make significant improvements in the process, it is essential to investigate the roles of convection in the PVT process.

Markham, Greenwell and Rosenberger [6] examined the effects of thermal and thermosolutal convections during the PVT process inside vertical cylindrical enclo-

†Corresponding author
Tel: +82-42-629-8837
Fax: +82-42-629-8835
E-mail: gtkim@hannam.ac.kr

sures for a time-independent system, and showed that even in the absence of gravity, convection can be present, causing nonuniform concentration gradients. They emphasized the role of geometry in the analysis of the effects of convection. As such these fundamentally constitute steady state two-dimensional models. The steady state models are limited to low Rayleigh number applications, because as the Rayleigh number increases oscillation of the flow field occurs. To address the issue of unsteady flows in PVT, Duval [7] performed a numerical study on transient thermal convection in the PVT processing of Hg_2Cl_2 very similar to the mercurous bromide for a vertical rectangular enclosure with insulated temperature boundary conditions for Rayleigh numbers up to 10^6. Nadarajah *et al.* [8] addressed the effects of solutal convection for any significant disparity in the molecular weights of the crystal components and the inert gas. Zhou *et al.* [9] reported that the traditional approach of calculating the mass flux assuming one-dimensional flow for low vapor pressure systems is indeed correct. Rosenberger *et al.* [10] studied three-dimensional numerical modeling of the PVT yielded quantitative agreement with measured transport rates of iodine through octofluorocyclobutane (C_4F_8) as inert background gas in horizontal cylindrical ampoules.

In this theoretical study, a two-dimensional model is used for the analysis of the PVT processes during vapor-growth of mercurous chloride crystals (Hg_2Cl_2) in horizontally oriented, cylindrical, closed ampoules in a two-zone furnace system. Diffusion-limited processes are considered in this paper, although the recent paper of Singh, Mazelsky and Glicksman [11] demonstrated that the interface kinetics plays an important role in the PVT system of Hg_2Cl_2. Thermally buoyancy-driven convection will be considered at this point even if a mixture of Hg_2Cl_2 vapor and impurity of Helium (He) would cause thermally and/or solutally buoyancy driven convection. Solutal convection would be negligible through $M_A = M_B$. In other words, for the density term and the binary diffusivity coefficient, the molecular weight of component B is set as that of component A intentionally.

It is the purpose of this paper to relate applied thermally buoyancy-driven convection process parameters such as thermal wall profiles (adiabatic and the linear temperature profiles at walls), temperature differences between the source and crystal region, aspect ratio (transport length-to-width) to the crystal growth rate and the maximum velocity magnitude to examine the effects of aspect ratio on thermally buoyancy-driven convection in order to gain insights into the underlying physicochemical processes.

2. Physical and Mathematical Formulations

Consider a rectangular enclosure of height H and transport length L, shown in Fig. 1. The source is maintained at a temperature T_s, while the growing crystal is at a temperature T_c, with $T_s > T_c$. PVT of the transported component A (Hg_2Cl_2) occurs inevitably, due to presence of impurities, with the presence of a component B (He). The interfaces are assumed to be flat for simplicity. The finite normal velocities at the interfaces can be expressed by Stefan flow deduced from the one-dimensional diffusion-limited model [12], which would provide the coupling between the fluid dynamics and species calculations. On the other hand, the tangential component of the mass average velocity of the vapor at the interfaces vanishes. Thermodynamic equilibria are assumed at the interfaces so that the mass fractions at the interfaces are kept constant at $\omega_{A,s}$ and $\omega_{A,c}$. On the vertical non-reacting walls appropriate velocity boundary conditions are no-slip, the normal concentration gradients are zero, and wall temperatures are imposed as nonlinear temperature gradients.

Thermophysical properties of the fluid are assumed to be constant, except for the density. When the Boussinesq approximation is invoked, density is assumed constant except the buoyancy body force term. The density is assumed to be a function of both temperature and concentration. The ideal gas law and Dalton's law of partial pressures are used. Viscous energy dissipation and the Soret-Dufour (thermo-diffusion) effects can be neglected, as their contributions remain relatively insignificant for the conditions encountered in our PVT crystal growth processes. Radiative heat transfer can be neglected under our conditions, based on Kassemi and

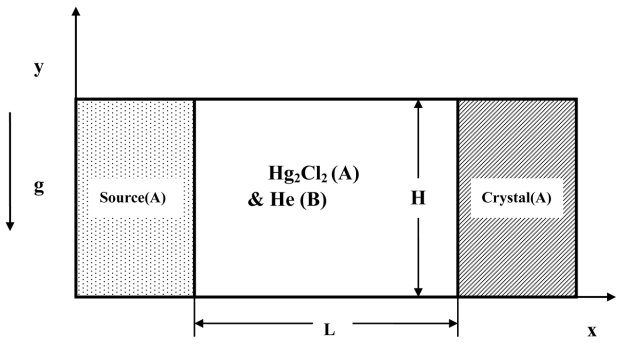

Fig. 1. Schematic of PVT growth reactor in a two-dimensional rectangular system.

Duval [13].

The transport of fluid within a rectangular PVT crystal growth reactor is governed by a system of elliptic, coupled conservation equations for mass (continuity), momentum, energy and species (diffusion) with their appropriate boundary conditions. Let v_x, v_y denote the velocity components along the x- and y-coordinates in the x, y rectangular coordinate, and let T, ω_A, p denote the temperature, mass fraction of species A (Hg_2Cl_2) and pressure, respectively.

The dimensionless variables are scaled as follows:

$$x^* = \frac{x}{H},\ y^* = \frac{y}{H}, \tag{1}$$

$$u = \frac{u_x}{U_c},\ v = \frac{v_y}{U_c},\ p = \frac{p}{\rho_c U_c^2}, \tag{2}$$

$$T^* = \frac{T-T_c}{T_s-T_c},\ \omega_A^* = \frac{\omega_A-\omega_{A,c}}{\omega_{A,s}-\omega_{A,c}}. \tag{3}$$

The dimensionless governing equations are given by:

$$\nabla^* \bullet V^* = 0, \tag{4}$$

$$\vec{V}^* \bullet \nabla^* \vec{V}^* = -\nabla^* p^* + Pr\nabla^{*2}\vec{V}^* - Ra \cdot Pr \cdot T^* \cdot e_g, \tag{5}$$

$$\vec{V}^* \bullet \nabla^* T^* = \nabla^{*2} T^* \tag{6}$$

$$\vec{V}^* \bullet \nabla^* \omega_A^* = \frac{1}{Le}\nabla^{*2}\omega_A^* \tag{7}$$

These nonlinear, coupled sets of equations are numerically integrated with the following boundary conditions:

On the walls ($0 < x^* < L/H$, $y^* = 0$ and 1):

$$u(x^*,0) = u(x^*,1) = v(x^*,0) = v(x^*,1) = 0 \tag{8}$$

$$\frac{\partial \omega_A^*(x^*,0)}{\partial y^*} = \frac{\partial \omega_A^*(x^*,1)}{\partial y^*} = 0,$$

$$T^*(x^*,0) = T^*(x^*,1) = \frac{T-T_c}{T_s-T_c}: \text{conducting}$$

$$\frac{\partial T^*(x^*,0)}{\partial y^*} = \frac{\partial T^*(x^*,1)}{\partial y^*} = 0: \text{adiabatic}$$

On the source ($x^* = 0$, $0 < y^* < 1$):

$$u(0,y^*) = -\frac{1}{Le(1-\omega_{A,s})}\frac{\Delta\omega}{\partial x^*}\frac{\partial \omega_A^*(0,y^*)}{\partial x^*}, \tag{9}$$

$$v(0,y^*) = 0,$$

$$T^*(0,y^*) = 1,$$

$$\omega_A^*(0,y^*) = 1.$$

On the crystal ($x^* = L/H$, $0 < y^* < 1$):

$$u(L/H,y^*) = -\frac{1}{Le(1-\omega_{A,c})}\frac{\Delta\omega}{\partial x^*}\frac{\partial \omega_A^*(L/H,y^*)}{\partial x^*} \tag{10}$$

$$v(L/H,y^*) = 0,$$

$$T^*(L/H,y^*) = 0,$$

$$\omega_A^*(L/H,y^*) = 0.$$

In the dimensionless parameters in the governing equations the thermophysical properties of the gas mixture are estimated from gas kinetic theory using Chapman-Enskog's formulas [14].

The vapor pressure [15] p_A of Hg_2Cl_2 (in the unit of Pascal) can be evaluated from the

$$p_A = e^{(a-b/T)}, \tag{11}$$

following formula as a function of temperature: in which a = 29.75, b = 11767.1.

The crystal growth rate V_c is calculated from a mass balance at the crystal vapor interface, assuming fast kinetics, i.e. all the vapor is incorporated into the crystal, which is given by (subscripts c, v refer to crystal and vapor respectively).

$$\int \rho_v \upsilon_v \cdot ndA = \int \rho_c \upsilon_c \cdot ndA, \tag{12}$$

$$\upsilon_c = \frac{\rho_v \int \upsilon_v \cdot ndA}{\rho_c \int dA}. \tag{13}$$

The detailed numerical schemes in order to solve the discretization equations for the system of nonlinear, coupled governing partial differential equations are found in [16].

3. Results and Discussion

One of the purposes for this study is to correlate the growth rate to process parameters such as an aspect ratio, adiabatic and linear thermal profiles at walls. Thus, it is desirable to express some results in terms of dimensional growth rate, however they are also applicable to parameter ranges over which the process varies in the manner given. The six dimensionless parameters, namely Gr, Ar, Pr, Le, C_v and Pe, are independent and arise naturally from the dimensionless governing equations and boundary conditions. The dimensionless parameters and physical properties for the operating conditions of this study are shown in Table 1.

When the molecular weight of a light element (He) is not equal to that of the crystal component (Hg_2Cl_2) during the physical vapor transport, both solutal and thermal effects should be considered. But, in this study, only thermally buoyancy-driven convection will be considered. The effects of solutal convection would be eliminated through $M_A = M_B$. In other words, for the density term and the binary diffusivity coefficient, the molecu-

Table 1
Typical thermo-physical properties used in this study (M_A = 472.086, M_B = 4.003)

Transport length, L	10 cm
Height, H	2 cm
Source temperature, T_s	450°C
Crystal temperature, T_c	430°C
Density, ρ	0.043 g/cm^3
Dynamic viscosity, μ	0.000325 g/(cm•sec)
Diffusivity, D_{AB}	0.0286 cm^2/s
Thermal expansion coefficient, β	0.00138 K^{-1}
Prandtl number, Pr	3.346
Lewis number, Le	0.078
Peclet, Pe	4.16
Concentration number, Cv	1.0158
Total system pressure, P_T	5401 Torr
Partial pressure of component B, P_B	50 Torr
Thermal Grashof number, Gr	4.83 × 10^5

lar weight of component B is set as that of component A intentionally. Note that in general, the insulated walls are difficult to obtain in practice and most of vapor growth experiments are performed under the imposed nonlinear thermal profile to avoid nucleation at the ampoule walls. To prevent undesirable nucleations at the walls, an often used experimental technique is to impose a nonlinear thermal profile with a maximum between the crystal and the source, and is usually referred to as a temperature "hump". This temperature hump could eliminate the problem of vapor supersaturation along the transport path and, thus, of parasitic nucleations at the walls. But, these humps may result in sharp temperature gradients near the crystal region, inducing thermal stresses and a decrease in crystal quality. In study, in order to investigate the effects of thermal convection on the physical vapor transport processes, the thermal wall boundary conditions such as adiabatic and the linear temperature profiles at walls are chosen intentionally for ground-based model study which would yield deep and thorough understandings of the essence of thermal convection through spaceflight experiments under microgravity experiments in near future.

Figure 2 shows the growth rates of Hg_2Cl_2 as a function of the temperature difference between the source and the crystal region, ΔT (K), for 10 K ≤ ΔT ≤ 50 K, T_s = 450°C, P_B = 50 Torr, Ar = 5, with adiabatic walls and horizontal orientation against the gravitational vector. For 10 K ≤ ΔT ≤ 50 K, the growth rate increases directly and linearly with increasing the temperature difference between the source and the crystal region. The rate is increased by a factor of 2 with increasing the temperature difference by a factor of 5. Therefore, the

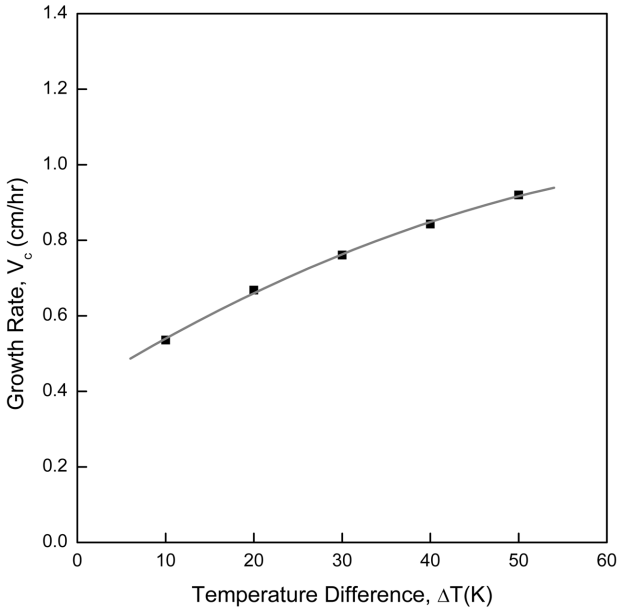

Fig. 2. Growth rates of Hg_2Cl_2 as a function of the temperature difference between the source and the crystal region, ΔT(K), for 10 K ≤ ΔT ≤ 50 K, T_s = 450°C, P_B = 50 Torr, Ar = 5, with adiabatic walls and horizontal orientation against the gravitational vector.

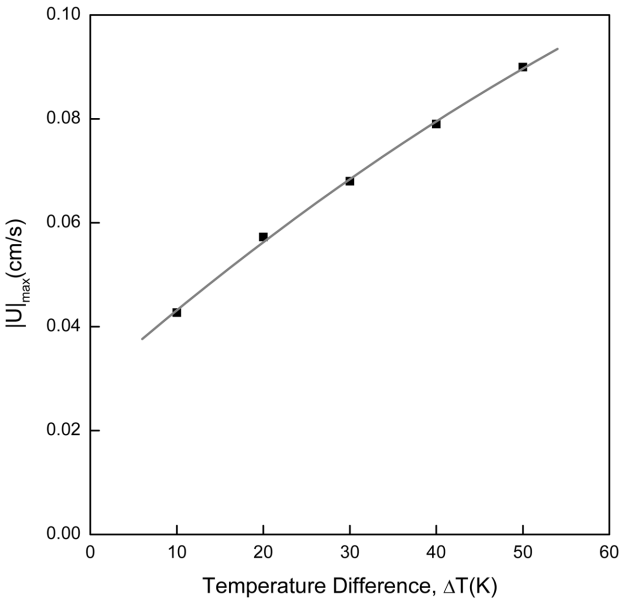

Fig. 3. The $|U|_{max}$ as a function of the temperature difference between the source and the crystal region, ΔT(K), corresponding to Fig. 2.

rate is considerably sensitive to the temperature difference, which reflects the low gradient of the rate-to-temperature difference. As shown in Fig. 3 corresponding to Fig. 2, the maximum magnitude of velocity vector which means the intensity of convection flows increases linearly with increasing the temperature difference, ΔT, for 10 K ≤ ΔT ≤ 50 K. The $|U|_{max}$ has a gradient of

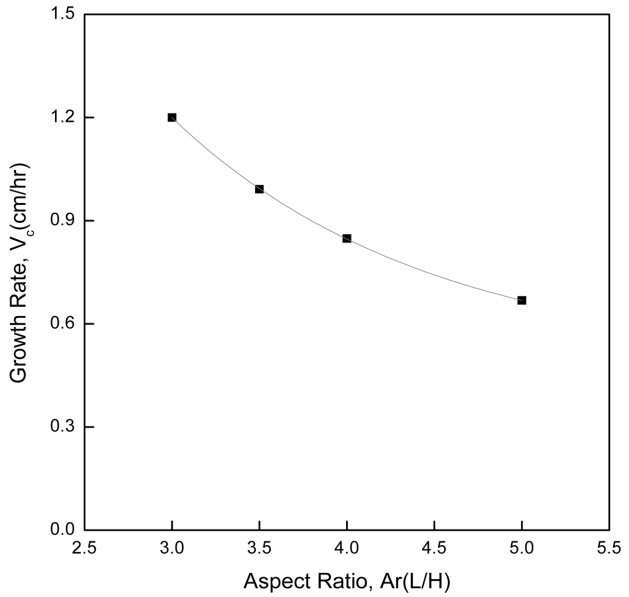

Fig. 4. Effects of aspect ratio Ar (L/H) on the crystal growth rates of Hg_2Cl_2, with the source region of the position fixed.

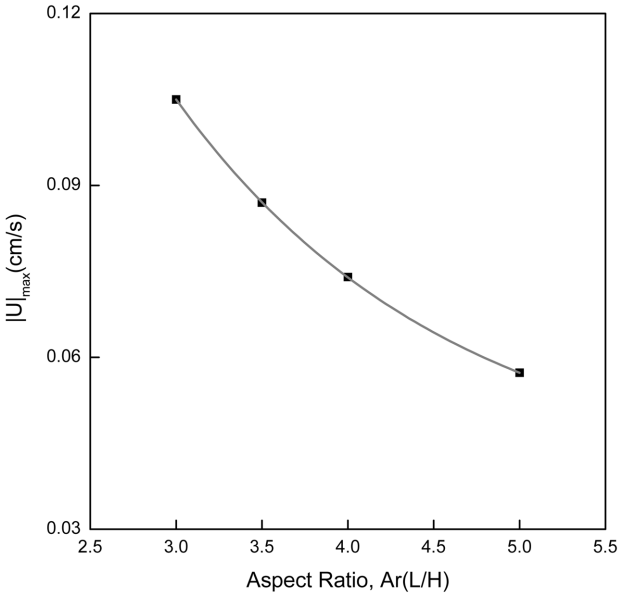

Fig. 5. The $|U|_{max}$ as a function of the aspect ratio Ar (L/H), corresponding to Fig. 4.

0.0011 cm/s•K, which reflects the importance of thermal convection. Figures 2 and 3 are based on 10 K ≤ ΔT ≤ 50 K, $T_s = 450^oC$, $P_B = 50$ Torr, Ar = 5, with adiabatic walls and horizontal orientation against the gravitational vector.

One now investigates the effects of the side walls on the growth rate and the maximum velocity magnitude of convective flow. Figure 4 shows the effects of aspect ratio, Ar (L/H) on the crystal growth rates of of Hg_2Cl_2, with the source region of the position fixed. Figure 4 are based on ΔT = 20 K, $T_s = 450^oC$, $P_B = 50$ Torr, P_T = 5401 Torr. For 3 ≤ Ar ≤ 5, the rate is decreased exponentially with increasing the aspect ratio, which indicates the role of kinetic effects on the crystal region as well as the effects of side wall. In particular, it is not surprising that the effects of side walls tend to stabilize convection in the growth reactor. This tendency is consistent with the results [18] on the pure thermal convection without crystal growth in enclosures. For ranges of convective parameters under consideration, the computer convergence for aspect ratios greater than 5 is difficult to obtain because of the high vapor pressure of mercurous chloride at the source region and possibility of the occurrence of turbulence. Figure 5 shows the relationship of $|U|_{max}$ and the aspect ratio, Ar (L/H). Considering Figs. 4 and 5, the side walls influence significantly on the rate and $|U|_{max}$. Therefore, the aspect ratio is also important in studying thermal convective effects.

As shown in Fig. 5, the maximum velocity magnitudes versus the aspect ratios show the same trend as

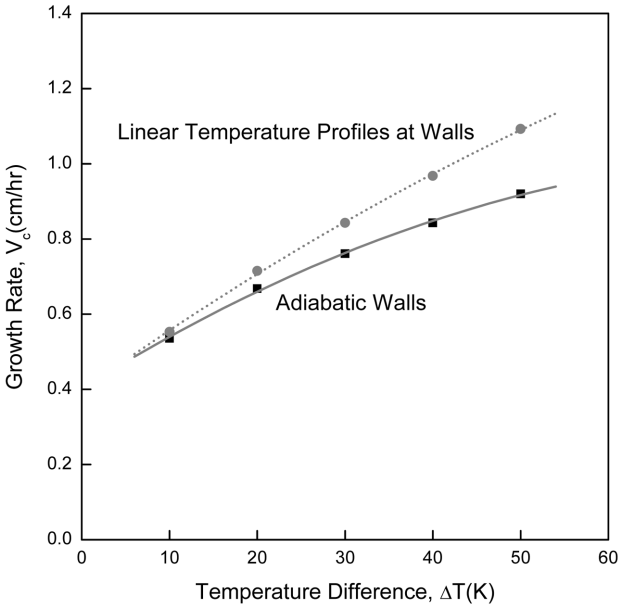

Fig. 6. Effects of the temperature difference on the crystal growth rates of Hg_2Cl_2, with the conducting and adiabatic walls for 10 K ≤ ΔT ≤ 50 K, $T_s = 450^oC$, $P_B = 50$ Torr, Ar = 5.

that versus the temperature difference shown in Fig. 4. In actual crystal growth system [19, 20], the temperature profile is intimately related to the aspect ratio because the temperature profile is so imposed that it could not be altered. In particular, for the temperature differences under considerations in this study, the aspect ratio is directly proportional to the temperature difference, with a fixed source region.

Figure 6 illustrates the effects of the temperature dif-

ference on the rate, with the conducting and the adiabatic walls for, ΔT (K), for $10\ K \le \Delta T \le 50\ K$, $T_s = 450^oC$, $P_B = 50$ Torr, Ar = 5. At the ranges of $10\ K \le \Delta T \le 10\ K$, the effect of the temperature difference has little influence on the two different wall boundary conditions. But, as the temperature difference increases, the rate is considerably influenced with the wall boundary conditions. For the ranges of the temperature difference, the rate for the linear temperature profile at walls, i.e., conducting walls is slightly greater than for the adiabatic walls.

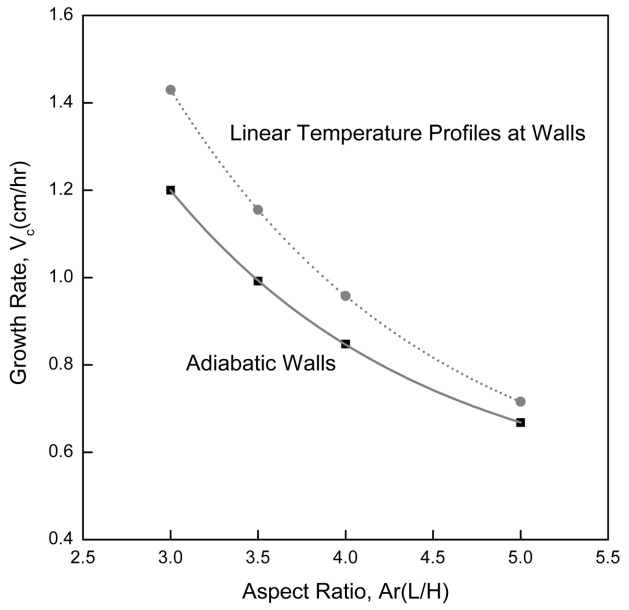

Fig. 7. Growth rates of Hg_2Cl_2 as a function of the aspect ratio Ar (L/H), with the conducting and adiabatic walls for $10\ K \le \Delta T \le 50\ K$, $T_s = 450^oC$, $P_B = 50$ Torr, Ar = 5.

As shown in Fig. 7, as the aspect ratio increases from 3.0 up to 5.0, the rate decays exponentially. The rate decreases exponentially with increasing the aspect ratio from 3.0 to 5 because of the effects of side walls. It should be noted that the temperature difference between the source and crystal region is fixed, i.e., T = 20 K. The effects of side walls are shown to be significant in the cases of the linear temperature profiles at walls and adiabatic walls. Note that because the vapor of component A (Hg_2Cl_2) is in a supersaturation throughout the ampoule, a linear temperature profile is rarely used in practice [8, 17].

Figure 8 shows the growth rates of Hg_2Cl_2 as a function of the dimensionless Peclet number, Pe, for $T_s = 450^oC$, $P_B = 50$ Torr, Ar = 5, with adiabatic walls. As the dimesionless Peclet number increases, the rate is increased linearly, which plays an important role on the thermal convection during the physical vapor transport of mercurosu chloride. The Peclet number reflects the intensity of condensation and sublimation at the crystal and source regions, respectively. The higher the Peclet number is, the greater the intensity of thermal convection is. The rate has a gradient of 0.177 cm/hr for the Peclet numbers under consideration. Figure 9 shows growth rates of Hg_2Cl_2 as a function of the dimension-

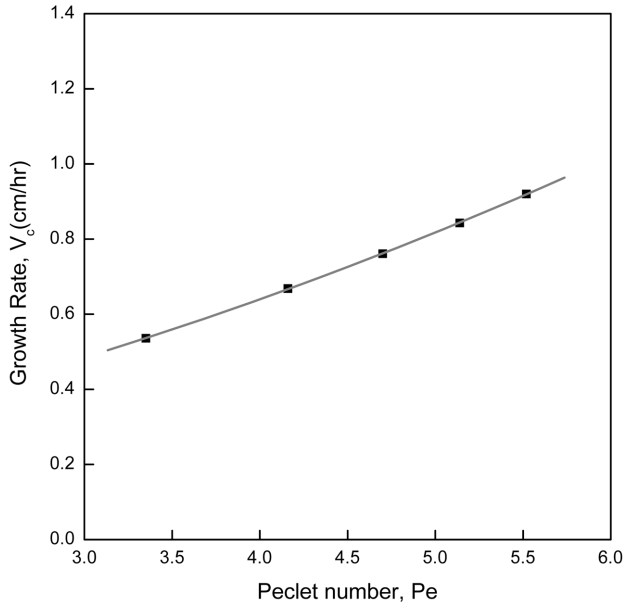

Fig. 8. Growth rates of Hg_2Cl_2 as a function of the dimensionless Peclet number, Pe, for $T_s = 450^oC$, $P_B = 50$ Torr, Ar = 5, with adiabatic walls and horizontal orientation against the gravitational vector.

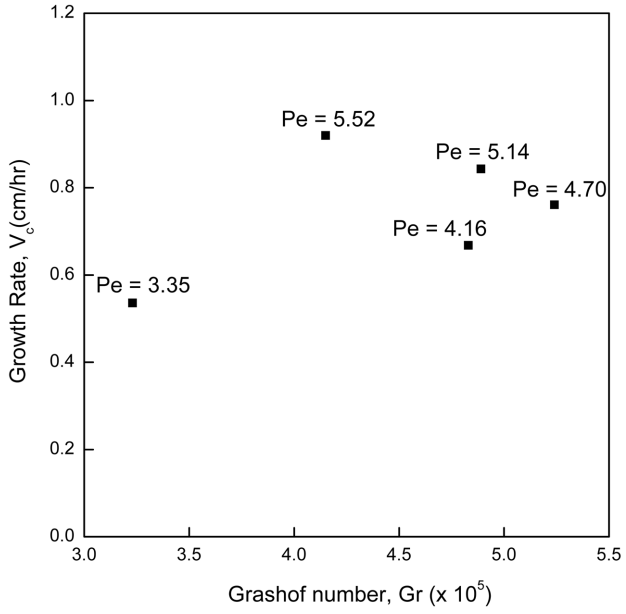

Fig. 9. Growth rates of Hg_2Cl_2 as a function of the dimensionless Grashof, Gr, for $T_s = 450^oC$, $P_B = 50$ Torr, Ar = 5, with adiabatic walls and horizontal orientation against the gravitational vector.

less Grashof, Gr, for $T_s = 450^oC$, $P_B = 50$ Torr, Ar = 5, with adiabatic walls. It is interesting that the rate is not linearly increased with the dimensionless Grashof number, Gr unlike the trend of the dimensionless Peclet number, Pe. The disparity in such a trend stems from the facts that an increase in the kinematic viscosity with increasing the temperature difference from 30 K to 50 K might result in a decrease in the dimensionless Grashof number from 5.24×10^5 to 4.15×10^5. Therefore, the growth rate are significantly influenced by the Grashof number as well as the Peclet number.

4. Conclusions

It is concluded that for an aspect ratio (transport length-to-width) of 5, Pr = 3.34, Le = 0.078, Pe = 4.16, Cv = 1.01, $P_B = 50$ Torr, only thermally buoyancy-driven convection ($Gr = 4.83 \times 10^5$) is considered in this study in spite of the disparity in the molecular weights of the component A (Hg_2Cl_2) and B which would cause thermally and/or solutally buoyancy-driven convection. The crystal growth rate and the maximum velocity vector magnitude are decreased exponentially for $3 \le Ar \le 5$, for (1) adiabatic walls and (2) the linear temperature profile, with a fixed source temperature. This is related to the finding that the effects of side walls tend to stabilize convection in the growth reactor. The rate for the linear temperature profiles walls is slightly greater than for the adiabatic walls for varied temperature differences and aspect ratios. With the imposed thermal profile, a fixed source region, both the rate and the maximum velocity vector magnitude increase linearly with increasing the temperature difference for $10 \le \Delta T \le 50$ K. At this point, a clear explanation on these phenomena of the relationship between Grashof number and the growth rate remains further study.

Acknowledgement

The authors wish to appreciate the financial support provided by the Hannam University through the Kyobi program of research project number of 2007A047 (April 1, 2007 through March 31, 2008).

References

[1] N.B. Singh, M. Gottlieb, G.B. Brandt, A.M. Stewart, R. Mazelsky and M.E. Glicksman, "Growth and characterization of mercurous halide crystals:mercurous bromide system," J. Crystal Growth 137 (1994) 155.
[2] N.B. Singh, R.H. Hopkins, R. Mazelsky and J.J. Conroy, "Purification and growth of mercurous chloride single crystals," J. Crystal Growth 75 (1970) 173.
[3] S.J. Yosim and S.W. Mayer, "The mercury-mercuric chloride system," J. Phys. Chem. 60 (1960) 909.
[4] F. Rosenberger, "Fluid dynamics in crystal growth from vapors," Physico-Chemical Hydro-dynamics 1 (1980).
[5] N.B. Singh, M. Gottlieb, A.P. Goutzoulis, R.H. Hopkins and R. Mazelsky, "Mercurous Bromide acousto-optic devices," J. Crystal Growth 89 (1988) 527.
[6] B.L. Markham, D.W. Greenwell and F. Rosenberger, "Numerical modeling of diffusive-convective physical vapor transport in cylindrical vertical ampoules," J. Crystal Growth 51 (1981) 426.
[7] W.M. B. Duval, "Convection in the physical vapor transport process-- I: Thermal," J. Chemical Vapor Deposition 2 (1994) 188.
[8] A. Nadarajah, F. Rosenberger and J. Alexander, "Effects of buoyancy-driven flow and thermal boundary conditions on physical vapor transport," J. Crystal Growth 118 (1992) 49.
[9] H. Zhou, A. Zebib, S. Trivedi and W.M.B. Duval, "Physical vapor transport of zinc-telluride by dissociative sublimation," J. Crystal Growth 167 (1996) 534.
[10] F. Rosenberger, J. Ouazzani, I. Viohl and N. Buchan, "Physical vapor transport revised," J. Crystal Growth 171 (1997) 270.
[11] N.B. Singh, R. Mazelsky and M.E. Glicksman, "Evaluation of transport conditions during PVT: mercurous chloride system," PhysicoChemical Hydrodynamics 11 (1989) 41.
[12] F. Rosenberger and G. Müller, "Interfacial transport in crystal growth, a parameter comparison of convective effects," J. Crystal Growth 65 (1983) 91.
[13] M. Kassemi and W.M.B. Duval, "Interaction of surface radiation with convection in crystal growth by physical vapor transport," J. Thermophys. Heat Transfer 4 (1989) 454.
[14] R.B. Bird, W.E. Stewart and E.N. Lightfoot, Transport Phenomena (New York, NY: John Wiley and Sons, 1960).
[15] C. Mennetrier and W.M.B. Duval, "Thermal-solutal convection with conduction effects inside a rectangular enclosure," NASA Technical Memorandum 105371 (1991).
[16] S. V. Patankar, Numerical Heat Transfer and Fluid Flow (Washington D.C.: Hemisphere Publishing Corp., 1980).
[17] G.T. Kim, "Convective-diffusive transport in mercurous chloride (Hg_2Cl_2) crystal growth ," J. Ceramic Processing Research 6 (2005) 110.
[18] I. Catton, "Effect of wall conducting on the stability of a fluid in a rectangular region heated from below," J. Heat Transfer 94 (1972) 446.
[19] N.B. Singh and W.M.B. Duval, "Growth kinetics of physical vapor transport processes: crystal growth of the optoelectronic material mercurous chloride," NASA Technical Memorandum 103788 (1991).
[20] C. Mennetrier, W.M.B. Duval and N.B. Singh, "Physical vapor transport of mercurous chloride under a nonlinear thermal profile," NASA Technical Memorandum 105920 (1992).